CHARACTERIZATION OF GYPSUM USING TMDSC

H. F. Dantas[1*]*, R. A. S. Mendes*[1]*, R. D. Pinho*[2]*, L. E. B. Soledade*[1]*, C. A. Paskocimas*[3]*,*
B. B. Lira[4]*, M. O. E. Schwartz*[2]*, A. G. Souza*[1] *and Iêda M. G. Santos*[1]

[1]Laboratório de Termoquímica e Materiais, Departamento de Química, CCEN, Universidade Federal da Paraíba, Campus I
58059-900 João Pessoa, PB, Brazil
[2]Departamento de Química Fundamental/Central Analítica, Universidade Federal de Pernambuco, 50740-540 Recife, PE, Brazil
[3]Departamento de Engenharia Mecânica, Universidade Federal do Rio Grande do Norte, Campus Universitário, 59072-970 Natal
RN, Brazil
[4]Laboratório de Materiais e Estruturas, Departamento de Engenharia Civil, CT, Universidade Federal da Paraíba, Campus I
58059-900, João Pessoa, PB, Brazil

Gypsum is a dihydrated calcium sulfate, with the composition of $CaSO_4 \cdot 2H_2O$, with large application interest in ceramic industry, odontology, sulfuric acid production, cement, paints, etc. During calcination, a phase transformation is observed associated to the loss of water, leading to the formation of gypsum or anhydrite, which may present different phases. The identification of the phases is not so easy since their infrared spectra and their X-ray diffraction patterns are quite similar. Thus, in this work, temperature modulated differential scanning calorimetry (TMDSC) was used to identify the different gypsum phases, which can be recognized by their different profiles.

Introduction

Pure gypsum, naturally existing in the nature as a somehow compact rock, is composed of calcium sulfate, displaying approximately 3% equilibrium moisture and about 20 mass% of chemically bound and/or combined crystallization water. Thus, its chemical formula is $CaSO_4 \cdot 2H_2O$ (calcium sulfate dihydrate) [1].

The thermal behavior of gypsum has been investigated due to its usage as a building material. During heating, gypsum undergoes two endothermic decompositions. The first dehydration reaction occurs at approximately 100–120°C, when calcium sulfate dihydrate is converted into calcium sulfate hemihydrate (the reaction is always complete at 160°C) as shown by Eq. (1) [2]:

$$CaSO_4 \cdot 2H_2O \rightarrow CaSO_4 \cdot 1/2H_2O + 3/2H_2O \qquad (1)$$
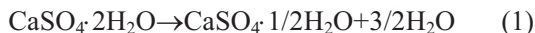
The amount of energy required by this first dehydration reaction is about 500 kJ kg^{-1} of gypsum.

The second dehydration reaction occurs when calcium sulfate hemihydrate is converted to anhydrous calcium sulfate, Eq. (2) [2]:

$$CaSO_4 \cdot 1/2H_2O \rightarrow CaSO_4 + 1/2H_2O \qquad (2)$$

The thermal decomposition of gypsum depends on the experimental conditions. Among these conditions, the heating rate and the atmosphere of the thermal treatment are particularly important. Thus, slow heating rates as well as low water vapor partial pres-

sures determine the formation of a product with a high specific surface area called to β-$CaSO_4$ III. The subsequent heating of this loose material leads to the compact α-$CaSO_4$ IV [2].

Two isostructural phases, α- and β-gypsum are frequently observed. The α-phase is prepared by the gypsum dehydration, in water-saturated environment, above 97°C. On the other hand, β-gypsum is obtained by heating at 100°C, in vacuum or under an unsaturated moisture environment. In relation to properties, the β-gypsum has a higher free energy and higher solubility than α-gypsum, leading to different properties during re-hydation. Therefore, α-gypsum requires less water to be re-hydrated than β-gypsum and its crystals do not disaggregate when they are placed to water [3–5].

In spite of the different properties α- and β-gypsum are difficult to be distinguished, due to their similar profiles when analyzed by X-ray diffraction and infrared spectroscopy. Hence, other techniques have been tested, to obtain fingerprints of these materials, using for instance the micro-Raman technique. In this work, natural gypsum was calcined at 170 and 400°C and characterized by the usual techniques and also by TMDSC.

Experimental

Ball milled as received gypsum, agricultural grade gypsum from the mine Rancharia – PE/Brazil was used

---

as raw material. In a laboratory electric rotary kiln ca. 300 g of the raw material were put into the oven and heated up to 170, 400 and 600°C at a heating rate of 50°C min^{-1}, and was kept under isotherm conditions for 30 min. Cooling occurred within the kiln by natural convection, upon switching off the furnace.

The samples were characterized before and after calcinations, using X-ray diffraction (D5000, Siemens), with CuK$_\alpha$ radiation, infrared spectroscopy using KBr pellets (MB 102, Bomem) and TMDSC (TA 2920 modulated DSC, TA Instruments). In these analyses, a sample mass of about 10 mg was used. The TMDSC analyses were carried out by scanning the samples in the 30–300°C temperature range, at an underlying heating rate of 10°C min^{-1} and a modulation amplitude of ±1.0°C every 60 s. Samples of α- and β-gypsum were also characterized for the sake of comparison.

Results and discussion

XRD patterns (Fig. 1) of the gypsum sample before heat treatment indicate the presence of gypsum dihydrate (JCPDS file 74-1433), besides the gypsum hemihydrate – the β-phase, with hexagonal structure and space group P-3m1 (JCPDS card 81-1848). After heating at 170°C, the amount of the dihydrate phase decreases, whereas the amount of β-gypsum increases. The same JCPDS files mentioned above were used to identify these phases. A small amount of anhydrite phase is already observed (JCPDS card 72-0916).

After calcination at 400°C, the dihydrate phase disappears. As expected, the amount of anhydrite (JCPDS card 72-0503) increases. In relation to hemihydrate, the diffractogram shows a superposition of two phases: β-gypsum (CaSO$_4\cdot$0.5H$_2$O – JCPDS card 14-0453) and another hydrated phase, with 0.67 mole of H$_2$O (CaSO$_4\cdot$0.67H$_2$O – JCPDS card 85-0531), with monoclinic structure.
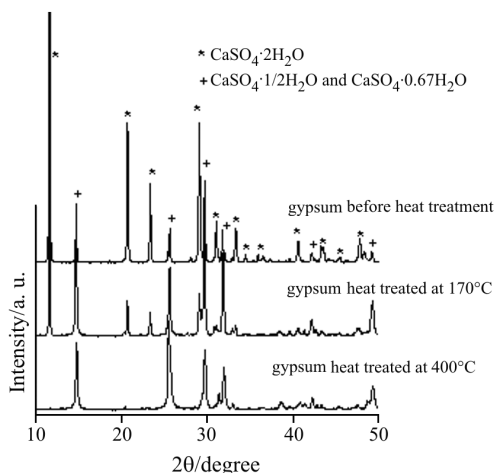

Fig. 1 XRD patterns of gypsum samples

A common structural motif in all CaSO$_4$ phases are chains in the form [–Ca–SO$_4$–Ca–SO$_4$–], where sulfate tetrahedra are coordinated through oxygen atoms with two neighboring Ca ions in the chain direction [6].

Gypsum is distinguished by a marked layer structure with perfect cleavability parallel to (010), where the sheets of coordinated water are located. The structure is monoclinic I2/a and is basically a layer structure bound together by hydrogen bonding. Zig-zag chains of CaO$_8$ polyhedra running parallel to the *c*-axis are bound together by similar zig-zag chains of SO$_4^{2-}$ units. This forms a double-sheet polyhedral layer perpendicular to the *b*-axe in which the two sheets are related by the *a*-glide. Two of the oxygen atoms bonded to the Ca^{2+} cations belong to H$_2$O molecules and the remaining six oxygen atoms are bonded to the sulfate groups. The H$_2$O molecules are significantly distorted and form a layer that binds together the polyhedral layers via the O–H hydrogen bond, which is directed almost entirely along the *b*-axis explaining the perfect {0 1 0} cleavage [7].

In the hemihydrate structure, the Ca^{2+} – SO$_4^{2-}$ chains run along the *c*-axis and form channels of approximately 4 Å diameter hosting the water molecules. Symmetry is near to a threefold screw axis. Deviations are obviously correlated with water content as discussed later. By means of careful drying of hemihydrate, water can be removed almost quantitatively, which yields the so-called soluble anhydrite (also denoted as AIII phase or γ-CaSO$_4$) with hexagonal symmetry. According to literature data, the α- and β-hemihydrates are not true polymorphs. The differences between them arise from their mode of production, resulting in different crystal sizes and habits, and not from different crystal structures [6, 8, 9].

The structure of the thermodynamically stable orthorhombic anhydrite (AII, insoluble anhydrite) contains the Ca–SO$_4$–Ca chains oriented in direction of the shorter *c*-axis. In *a*- and *b*-direction these chains are corner-linked [6].

Therefore, it may be observed that the X-ray diffraction patterns may not lead to the complete elucidation of the phases present in gypsum samples. This fact is due to the different gypsum phases, which show superposition of peaks, making the identification difficult. For α- and β-phases, the problem is even more difficult, once they present the same crystal structure.

An important point is the presence of dihydrate phases even after calcination at 170°C, indicating that the dehydration reaction was not complete.

Infrared spectra were used to evaluate the gypsum samples before and after thermal treatment. The results are presented in Fig. 2.
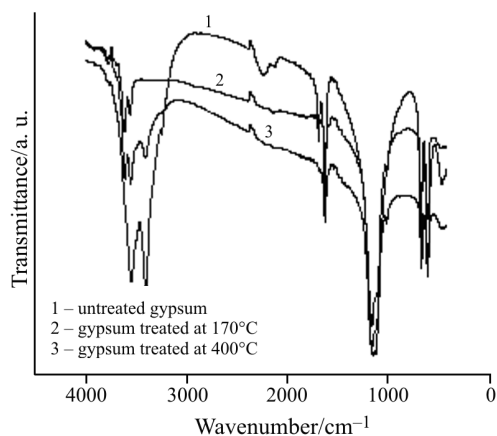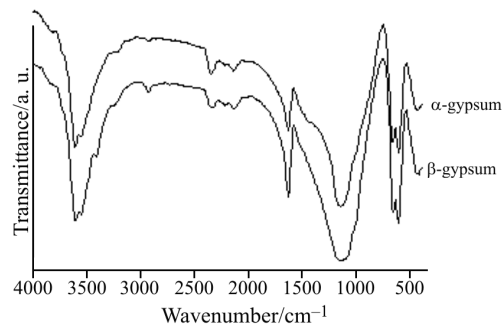
Fig. 2 Infrared spectra of the untreated and heat treated gypsum samples

Fig. 3 Infrared spectra of α- and β-gypsum samples

According to the literature, the observed spectra are characteristic of calcium sulfate [10]. Three sulfate bands are observed, ν_2 is a small band around 460 cm^{-1}, which becomes broader after calcination, ν_3 is a broad band located at about 1150 cm^{-1}, while ν_4 band splits into two bands at about 600 and 660–670 cm^{-1}. The lattice water absorbs at 3400–3600 cm^{-1} (antisymmetric and symmetric OH stretchings) and at 1620–1685 cm^{-1} (HOH bending). For natural gypsum, another band at about 2120–2232 cm^{-1} is also observed, indicating the presence of contamination [11, 12].

The main differences between the three spectra are related to water bands. The bands at 3404 and 1684 cm^{-1} disappear after heat treatment at 400°C, while the band at 3540 cm^{-1} dislocates to higher frequencies ($\Delta\nu=10$ cm^{-1}).

The spectra of calcined gypsum were compared to known samples of α- and β-gypsum (Fig. 3). A similar profile is observed for all samples analyzed, with small differences in the position of the bands. These results show that differentiation between α- and β-forms of gypsum using infrared spectroscopy is rather difficult.

DTA is a useful technique to characterize the different forms of gypsum. In general, all of the studies of CaSO$_4$·2H$_2$O dehydration using DTA show the presence of the two endothermic peaks. However, the corresponding temperatures show remarkable alteration: these peaks were obtained at 130 and 180, 180 and 215 or 149 and 169°C, for example. They indicate the crystal structure modification. According to Sebbahi and Elbeyli [13, 14], the corresponding temperatures are influenced by the experimental conditions, e.g. by the heating rate, nitrogen or air atmosphere and sample impurities. Another important point is the influence of nature as well as the different origin of the samples.

The next peak is exothermic, indicating the transition of soluble γ-anhydrite (with hexagonal structure) to insoluble β-anhydrite (with orthorhombic structure). The temperature of this peak depends on the precursor. For natural gypsum, the previous reactions lead to the formation of β-gypsum, which transforms to γ-anhydrite and to β-anhydrite above 350°C. The same temperature range is observed in the DTA curves of β-gypsum. When α-gypsum is evaluated, a very sharp exothermic peak appears at lower temperatures, around 215°C [4, 13, 15].

When the thermal analysis is performed by TMDSC, the reversing and non-reversing events are separated. These results are presented in Fig. 4.

The reversing curves present one to four endothermic peaks and one exothermic peak, depending on the heat treatment. These peaks might be related to phase
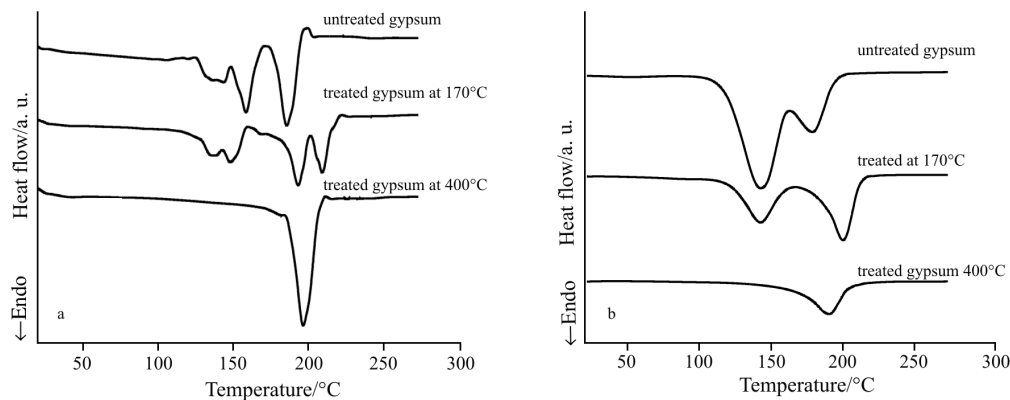
Fig. 4 a – Reversing and b – non-reversing TMDSC curves of untreated and heat treated gypsum samples

transitions. The non-reversing curves display one or two endothermic peaks, according to the heat treatment. These peaks are related to dehydration processes.

When the endothermic peak in the non-reversing curve is related to one peak in the reversing curve, probably phase transition associated to dehydration process occurs. These transitions are currently observed in the DTA curves as stated before. In the present case, the untreated samples and the samples after calcination at 170°C present two steps with these characteristics – the first one at about 145°C (assigned to the Eq. (1)) and the second one at about 180°C (assigned to the Eq. (2)) for the untreated sample and at about 195°C for the sample calcined at 170°C. After calcination at 400°C, a dehydration process still occurs at about 190°C. According to Chang *et al.*, $CaSO_4$ might absorb moisture, leading to the sample re-hydration [12].

Reversing curves display two other endothermic and one exothermic peaks, which are not related to the dehydration processes. According to Angeleri and Cardoso [3–5], gypsum presents at least nine different crystalline phases: two with the composition of $CaSO_4·2H_2O$, three phases with composition of $CaSO_4·1/2H_2O$ and four phases with composition of $CaSO_4$. Thus, these peaks may be related to phase transitions which are not related to a dehydration process. The endothermic transition at 136°C, present in the untreated and treated at 170°C samples, may be assigned to a phase transition of the gypsum di-

hydrate. The endothermic transition of untreated gypsum, observed at 158°C, may be assigned to a transition of the hemihydrated gypsum. The endothermic peak observed at 209°C in the gypsum heat treated at 170°C and the exothermic peaks noticed in this sample are related to transitions of the anhydrite.

According to Angeleri *et al.* [4], one exothermic peak is observed at 215 and 360°C for α- and β-gypsum, respectively, and it is related to the γ-anhydrite→β-anhydrite transition. When natural gypsum is studied by DTA, this peak is observed at about 360°C, due to the analysis conditions (opened crucible). In the present case, closed crucibles are used in the analyses. So, the exothermic peak is observed at lower temperature, indicating that α-gypsum is formed during the decomposition process. The highest intensity of the exothermic peak, observed for untreated gypsum, indicates that a higher amount of α-gypsum is formed in this sample.

The TMDSC curves of the analyzed samples were compared to the TMDSC curves of α- and β-gypsum and anhydrite and are displayed in Fig. 5. The reversing curves of are different – α-gypsum presents two endothermic peaks with similar intensities, while β-gypsum presents a small endothermic peak followed by a high intensity peak. The non-reversing curves of both gypsum forms present one endothermic peak, but only α-gypsum presents one exothermic peak just after the endothermic peak.
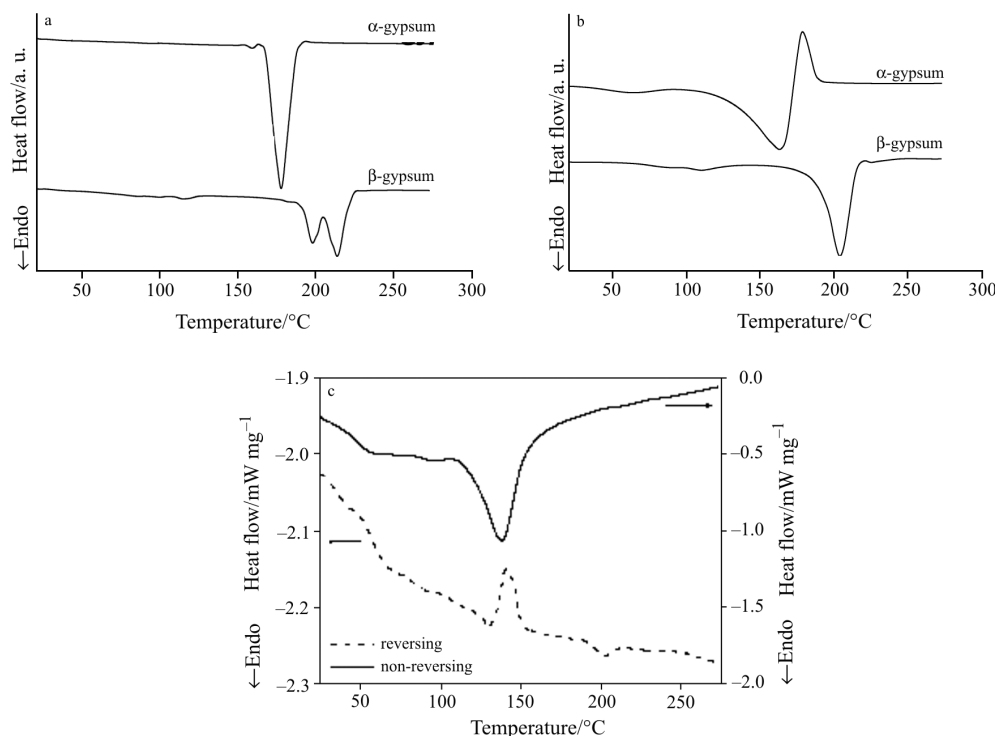

Fig. 5 TMDSC curves of α-, β-gypsum and anhydrite samples; a – reversing, b – non-reversing and c – anhydrite

This result indicates that β-gypsum is formed after heat treatment at 170°C, besides gypsum dihydrate, in agreement with the XRD patterns. After calcination at 400°C, XRD patterns indicate that anhydrite and hemihydrate phase are formed. TMDSC results show that the non-reversing profile is very similar to the β-phase, as α-gypsum presents a sharp exothermic peak after the endothermic peak. On the other hand, the reversing curve shows a small endothermic peak at 178°C and a larger peak at 196°C. The small endothermic peak may due to the superposition of the exothermic one, characteristic to the anhydrite, as presented in Fig. 5. Thus, the TMDSC results indicate that β-gypsum is formed after heat treatment at 170 and 400°C.

Conclusions

The obtained results indicate that TMDSC can be used to identify the different forms present in gypsum samples, completed with X-ray diffraction. A clear difference is observed between the reversing and the non-reversing curves of α- and β-gypsum, making the identification easier. In the present case, the heat treatment leads to the formation of β-gypsum.

Another important point is the possibility of identification of other phase transitions, which are not related to the dehydration processes. Due to their superposition with dehydration peaks, these transitions cannot be observed using conventional DTA/DSC analysis.

Acknowledgements

References

1 A. Belmiloudi and G. Le Meur, Appl. Math. Comput., 163 (2005) 1023.
2 D. Fatu, J. Therm. Anal. Cal., 65 (2001) 213.
3 F. B. Angeleri and S. R. F. Cardoso, Cerâmica, 28 (1982) 156.
4 F. B. Angeleri and S. R. F. Cardoso, Cerâmica, 29 (1983) 157.
5 F. B. Angeleri and S. R. F. Cardoso, Cerâmica, 29 (1983) 190.
6 D. Freyer and W. Voigt, Monatsh. Chem., 134 (2003) 693.
7 P. F. Schofield, I. C. Stretton, K. S. Knight and S. Hull, Physica B, 234–236 (1997) 942.
8 A. J. Lewry and J. Williamson, J. Mater. Sci., 29 (1994) 5279.
9 R. J. Hand, Br. Ceramic, 96 (1997) 116.
10 R. Nyquist and R. Kagel, Infrared Spectra of Inorganic Compounds, Academic Press, San Diego 1971.
11 K. Nakamoto, Infrared and Raman Spectra of Inorganic and Coordination Compounds, John Wiley & Sons, New York 1986.
12 H. Chang, P. J. Huang and S. C. Hou, Mater. Chem. Phys., 58 (1999) 12.
13 S. Sebaahi, M. L. O. Chameikh, F. Sahban, J. Aride, L. Benarafa and L. Belfbir, Thermochim. Acta, 302 (1997) 69.
14 I. Y. Elbeyli, E. M. Derun, J. Gülen and S. Piskin, Cem. Concr. Res., 33 (2003) 1729.
15 I. Y. Elbeyli and S. Piskin, J. Hazard. Mater., B116 (2004) 111.